

This article was downloaded by: [Universita di Palermo]

On: 29 September 2014, At: 08:56

Publisher: Taylor & Francis

Informa Ltd Registered in England and Wales Registered Number: 1072954 Registered office: Mortimer House, 37-41 Mortimer Street, London W1T 3JH, UK



## Journal of Hydraulic Research

Publication details, including instructions for authors and subscription information:  
<http://www.tandfonline.com/loi/tjhr20>

### Storm sewer pressurization transient - an experimental investigation

Giovanni B. Ferreri Associate Professor<sup>a</sup>, Giuseppe Ciraolo Assistant Professor<sup>b</sup> & Carlo Lo Re Research Assistant<sup>c</sup>

<sup>a</sup> Dipartimento di Ingegneria Civile, Ambientale, Aerospaziale, dei Materiali, Università degli Studi di Palermo, Viale delle Scienze - Ed. 8, IT-90128 Palermo, Italy

<sup>b</sup> Dipartimento di Ingegneria Civile, Ambientale, Aerospaziale, dei Materiali, Università degli Studi di Palermo, Viale delle Scienze - Ed. 8, IT-90128 Palermo, Italy

<sup>c</sup> Dipartimento di Ingegneria Civile, Ambientale, Aerospaziale, dei Materiali, Università degli Studi di Palermo, Viale delle Scienze - Ed. 8, IT-90128 Palermo, Italy

Published online: 17 Jul 2014.

To cite this article: Giovanni B. Ferreri Associate Professor, Giuseppe Ciraolo Assistant Professor & Carlo Lo Re Research Assistant (2014): Storm sewer pressurization transient - an experimental investigation, Journal of Hydraulic Research, DOI: [10.1080/00221686.2014.917726](https://doi.org/10.1080/00221686.2014.917726)

To link to this article: <http://dx.doi.org/10.1080/00221686.2014.917726>

PLEASE SCROLL DOWN FOR ARTICLE

Taylor & Francis makes every effort to ensure the accuracy of all the information (the "Content") contained in the publications on our platform. However, Taylor & Francis, our agents, and our licensors make no representations or warranties whatsoever as to the accuracy, completeness, or suitability for any purpose of the Content. Any opinions and views expressed in this publication are the opinions and views of the authors, and are not the views of or endorsed by Taylor & Francis. The accuracy of the Content should not be relied upon and should be independently verified with primary sources of information. Taylor and Francis shall not be liable for any losses, actions, claims, proceedings, demands, costs, expenses, damages, and other liabilities whatsoever or howsoever caused arising directly or indirectly in connection with, in relation to or arising out of the use of the Content.

This article may be used for research, teaching, and private study purposes. Any substantial or systematic reproduction, redistribution, reselling, loan, sub-licensing, systematic supply, or distribution in any form to anyone is expressly forbidden. Terms & Conditions of access and use can be found at <http://www.tandfonline.com/page/terms-and-conditions>



Research paper

## Storm sewer pressurization transient – an experimental investigation

GIOVANNI B. FERRERI, Associate Professor, *Dipartimento di Ingegneria Civile, Ambientale, Aerospaziale, dei Materiali, Università degli Studi di Palermo, Viale delle Scienze - Ed. 8, IT-90128 Palermo, Italy*

Email: [giovannibattista.ferreri@unipa.it](mailto:giovannibattista.ferreri@unipa.it) (author for correspondence)

GIUSEPPE CIRAOLO, Assistant Professor, *Dipartimento di Ingegneria Civile, Ambientale, Aerospaziale, dei Materiali, Università degli Studi di Palermo, Viale delle Scienze - Ed. 8, IT-90128 Palermo, Italy*

Email: [giuseppe.ciraolo@unipa.it](mailto:giuseppe.ciraolo@unipa.it)

CARLO LO RE, Research Assistant, *Dipartimento di Ingegneria Civile, Ambientale, Aerospaziale, dei Materiali, Università degli Studi di Palermo, Viale delle Scienze - Ed. 8, IT-90128 Palermo, Italy*

Email: [carlo.lore@unipa.it](mailto:carlo.lore@unipa.it)

### ABSTRACT

Pipe pressurization is examined experimentally by 144 laboratory experiments in a circular tilting pipe between two tanks, in which the transient was triggered by sudden closing of the downstream tank outlet. The experiments cover ranges of values of slope, velocity and filling ratio of the open-channel flow not explored in previous studies. Situations involving considerable air quantity and consequent intense pressure oscillations were also reproduced. Two different pressurization patterns, defined as “smooth” and “abrupt”, were observed, but only the abrupt pattern produced intense pressure oscillations. The comparison among all the abrupt pressurization surges showed how the oscillations changed in starting time, intensity and duration as the pipe slope, the flow rate and the free-surface flow filling ratio varied. The experimental results also stressed the major role of entrapped air in determining the oscillation characteristics, showing that oscillations were actually produced by the pulsating of large air pockets during their migration along the pipe and their release through the upstream manhole.

*Keywords:* Air–water flow; pressurization; storm sewer system; transition; unsteady flow; urban drainage

### 1 Introduction

Urban drainage networks are usually designed to operate in a free-surface condition, with filling ratios up to 0.7–0.8. However, as a consequence of severe rainfall events, even not exceptional ones, either the water volumes and/or the times in which they concentrate or network malfunctioning (e.g. pipe obstruction, back flow from the downstream conduit or pump stop) can cause sewer filling and network overflowing, with flooding of streets and cellars. During transition from free-surface to pressurized flow, air present in sewers can be entrapped in the liquid flow in the form of pockets, even large ones, on the sewer crown (Hamam and McCorquodale 1982, Zhou *et al.* 2002b, Vasconcelos and Wright 2005, Ciraolo and Ferreri 2007). The pockets then move along the sewers to be finally released through the vented manholes.

Sewer pressurization can generate non-negligible pressure oscillations that are capable of damaging the network (Song 1976, Hamam and McCorquodale 1982, Song *et al.* 1983, Li and

McCorquodale 1999, Zhou *et al.* 2002a). According to Hamam and McCorquodale (1982), for a free-surface flow velocity of  $1.5 \text{ m s}^{-1}$ , pressurization surcharges of 6–40 m may occur in real culverts. Zhou *et al.* (2002a) reported that a 12–15 m surcharge was estimated in a real storm system severely damaged during an extreme storm. As a consequence of pressurization, raising or ejection of manhole covers is often observed (Hamam and McCorquodale 1982, Guo and Song 1991) and sometimes formation of geysers (i.e. intermittent air–water jets in the atmosphere) (Guo and Song 1990, 1991).

The pressurization most usually studied is that produced by a drastic reduction in the discharge at the end section of a sewer, which causes a rapid rise in the free-surface and the formation of a bore that moves upstream. The formation of the bore front and the surge following the passing of the bore were studied experimentally and numerically by several researchers (Wiggert 1972, Hamam and McCorquodale 1982, Cardle *et al.* 1989, Li and McCorquodale 1999, Trajkovic *et al.* 1999). Pressurization surge was also studied, but only numerically, by Song (1976)

Received 10 August 2012; accepted 20 April 2014/Currently open for discussion.

and Song *et al.* (1983) who, however, aimed at mathematical modelling of network pressurization, not at investigation of the physical phenomena occurring in a single sewer that pressurizes.

As for the central topic of pressure oscillations, some authors (Hamam and McCorquodale 1982, Cardle *et al.* 1989, Li and McCorquodale 1999, Aimable and Zech 2003) imputed their start to the formation of free-surface instability caused by the overhanging “wind” driven by the advancing bore; according to Cardle *et al.* (1989), oscillations vanished when the bore front flowed into the upstream tank. Other experiments carried out by Vasconcelos and Wright (2005) and Zhou *et al.* (2002a, 2002b) addressed flow initiation and pipe filling, respectively, and showed that: (a) intense pressure oscillations occurred during air release and (b) pressure oscillations had different characteristics depending on the amount of air and the ease of release. Few additional studies are found in the technical literature.

Despite awareness of the complexity of pressurization and concern about its possible consequences, this transient is still little understood, both qualitatively and quantitatively because pressurization has been studied in only a few experiments, each aiming to reproduce some designated aspect of the transient (e.g. front formation, pressure oscillation start, link between air release and oscillations). In some cases (Capart *et al.* 1997, Trajkovic *et al.* 1999), the experiments aimed at validating the numerical results of mathematical models based on de Saint-Venant’s equations with the help of the Preissmann slot; therefore, for these equations to remain valid, the researchers appropriately considered experimental situations (namely, low values of flow rate, velocity and filling ratio) that involved neither considerable air participation nor appreciable pressure oscillations. However, the spread of drainage network mathematical models, with increasing importance of physically based ones, now requires investigation of sewer pressurization as a whole, considering experimental situations reproducing all phenomena to correctly model the whole transient.

Such comprehensive testing was carried out at the University of Palermo (Italy), and the main results are reported here. A tilting circular pipe between two tanks was used that had a diameter of about 250 mm and a length of 26 m. The diameter was noticeably larger than those used in previous literature experiments (usually ranging between 90 and 150 mm), an important feature when investigating pressurization phenomena concurrently because phenomena such as flow turbulence, air entrainment, bubble motion, free-surface instability and others are not scaled

as much as inertial force and gravity force when transferring from a field system to a laboratory system.

The experiments (144 in total) explored pressurization through 48 combinations of slope and flow rate, which varied by constant steps to detect any change in the pressurization phenomena. On the whole, this practice produced values of slope, velocity and filling ratio of the free-surface flow varying within considerably larger ranges than those studied in the literature, to reproduce situations involving even considerable air participation.

## 2 Experimental equipment and procedures

The experimental facility (Fig. 1) consisted of a Plexiglas circular pipe between two steel tanks. The pipe was 26.09 m long and had an internal diameter  $D = 244$  mm and a slope  $S_0$  adjustable in the range 0–3%. Plexiglas allowed us to observe the phenomena inside the pipe, facilitating interpretation of the measurements recorded by the acquisition system.

The upstream tank (Fig. 2a) consisted of two chambers 40 cm wide linked by a short circular pipe close to the bottom with the same diameter as the experimental pipe. The first chamber functioned to calm the water before it entered the second chamber. Water was supplied by a vertical pipe entering the chamber through a watertight hole in the bottom. The second chamber, analogous to a real culvert manhole, had a  $U$ -shaped bottom, with side sloped benches; the  $U$ -gutter was as wide as the experimental pipe and was aligned with both the experimental pipe and the link pipe so that flow contraction was practically eliminated for depths lower than half the diameter and noticeably reduced for higher depths. To adjust the depth of the open-channel flow entering the experimental pipe without choking the pipe inlet, a sharp sluice-gate was located at the inlet of the short pipe linking the two chambers. Each chamber had a spillway located as shown in the figure, with the aim of stopping the water level rise after pipe pressurization.

The downstream tank (Fig. 2b) was rectangular and 40 cm wide. The wall opposite the pipe outlet could be located in three positions,  $A$ ,  $B$  and  $C$ , respectively about 29, 14.5 and about 0 cm from the pipe outlet; consequently, the tank capacity could, respectively, be about 120, 60 and 0 dm<sup>3</sup>, allowing us to compare the transient characteristics for different tank capacities (the rise-rate of the tank level changed). In the lower part of the movable

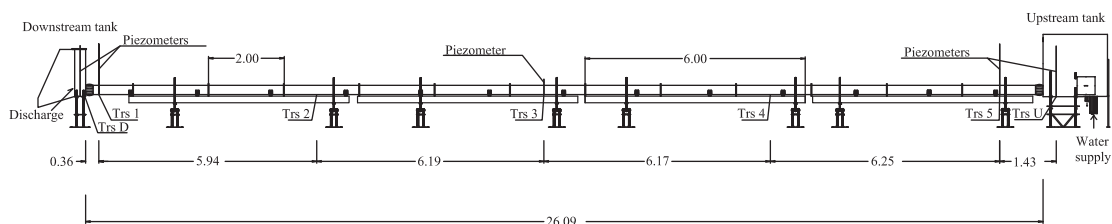


Figure 1 Experimental facility, with transducer locations (Trs 1–5) along the pipe from the downstream tank to the upstream tank. Distances are given in meters

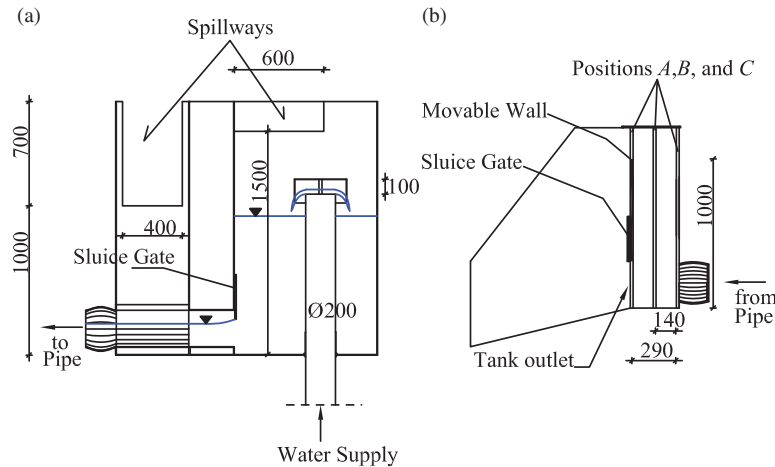


Figure 2 Longitudinal sections of the (a) upstream tank with water inlet and sluice-gate, and (b) downstream tank with movable wall positions *A*, *B* and *C*

Table 1 Hydraulic characteristics for each run cycle I–VI

Cycle	$S_0$ (%)	$Q$ ( $\text{dm}^3 \text{s}^{-1}$ )	$y_1/D$	$V_1$ ( $\text{m s}^{-1}$ )	$F_1$
I	0.2	15–40	0.434–0.787	0.77–1.01	0.866–0.728
II	0.6	15–40	0.311–0.545	1.21–1.54	1.64–1.50
III	1.0	25–65	0.369–0.631	1.60–2.09	1.98–1.84
IV	1.5	25–65	0.336–0.545	1.81–2.49	2.37–2.43
V	2.0	25–65	0.316–0.525	1.98–2.62	2.67–2.62
VI	2.5	25–65	0.295–0.496	2.17–2.81	3.04–2.91

wall, aligned with the pipe outlet, there was a 25 cm square-intake that could be closed by a sharp sluice-gate. The sluice-gate closing caused rapid filling of the tank and bore formation, which initiated the pipe pressurization. The movable wall, with a crest 1 m above the bottom, could be overflowed. The play of the tracks where the movable wall and the sluice-gate were seated allowed side water leaks to occur. Moreover, when the movable wall was in position *C*, the short distance left between it and the fixed wall allowed water to flow between the two walls and to overflow the wall crest.

The apparatus (Fig. 1), with the upstream and downstream spillways placed 1 m from the respective bottoms, outlined a sewer conduit between two manholes; the beginning of the spillway operation simulated the street flooding. The downstream spillway operated in all the runs, whereas the upstream spillway (only the lower one) operated (a) for all the runs relating to the position *C* of the movable wall and (b) for several of the other runs according to the flow rate and the pipe slope.

The flow rate entering the system was gauged by an electromagnetic meter. Pressure gauging was made by seven transducers (five along the pipe and one in each tank), whose locations and serial numbers are shown in Fig. 1. During steady free-surface flow before pressurization, the pipe flow depth was gauged in the sections indicated in Fig. 1 by piezometers equipped by point-gauges with a 1/10 mm nonius. Two analogous piezometers gauged the steady tank water levels before and

after pressurization. In all runs, the pressurization was initiated by letting the downstream tank sluice-gate fall freely.

The runs (Table 1) were organized in six *cycles* (denoted as I–VI), each relating to a value of the pipe slope  $S_0$  ranging between 0.2% and 2.5%. Each cycle included three run *groups* according to the position *A*, *B* or *C* of the downstream tank movable wall. For each group, from six to nine flow rates increasing by steps of  $5 \text{ dm}^3 \text{ s}^{-1}$  were tested. In total, 144 runs were performed, with a flow rate  $Q = 15 - 65 \text{ dm}^3 \text{ s}^{-1}$  and free-surface flow having a filling ratio  $y_1/D \approx 0.3 - 0.8$  ( $y_1$  being the flow depth), velocity  $V_1 \approx 0.79 - 2.8 \text{ m s}^{-1}$  and Froude number  $F_1 \approx 0.7 - 3$ . The latter was computed by  $F_1 = V_1/\sqrt{gA_1/B_1}$ , where  $A_1$  is the cross-sectional area,  $B_1$  the free-surface width and  $g$  the gravity acceleration. The filling ratio  $y_1/D$  was always  $< 0.81$ , which is the limit for any free-surface instability to not evolve into pipe pressurization (Hamam and McCorquodale 1982, Cardle *et al.* 1989).

The runs were performed according to the following procedure. For fixed slope (run cycle) and movable wall position (run group), the sluice-gate of the downstream tank was completely opened while the sluice-gate of the upstream tank was regulated (as specified later); then the flow rate was set. When steady flow conditions settled, the flow depths in sections *a*, *b* and *c* were gauged to check that no marked differences existed among them, and the depth in section *b* (pipe middle) was assumed as flow depth  $y_1$  to calculate  $y_1/D$ ,  $V_1$  and  $F_1$ . The acquisition system was

then started, and the downstream sluice-gate was allowed to fall freely, initiating the pressurization transient; the transient ended when the upstream tank level steadied. Finally, the downstream sluice-gate was suddenly opened, starting pipe depressurization and restoration of the initial flow conditions.

The opening of the sluice-gate between the two chambers of the upstream tank was set such that the free-surface flow depth  $y_1$  was close to the flow rate normal depth; the flow rate normal depth was determined using the Manning's roughness coefficient  $0.010 \text{ s m}^{-1/3}$  previously obtained experimentally. In practice, the opening height was set at that of the fixed values 12.5, 15.5, 18.5, 21.5 and 25 cm which was higher than the normal depth divided by the contraction coefficient 0.6.

Film clips taken of each run were used as a basic tool to closely observe the phenomena. Repeated film clip reproductions allowed us to develop a more accurate description of pressurization and a robust explanation of the measured pressure oscillations in the light of the observed phenomena.

### 3 Experimental results

The numerous runs performed (48 combinations of slope and flow rate for each movable wall position) allowed various behaviours to be observed, although many were specific to a few runs only. For the sake of brevity, only the most common behaviours observed in the complete runs will be discussed here.

#### 3.1 Pressurization patterns

Pressurization occurred following two distinct patterns, depending on the flow rate,  $Q$ . For the lower flow rates, the front consequent on the closing operation did not reach the pipe crown (Fig. 3a), and a bore began to migrate upstream along the pipe (Fig. 3b), causing a sudden rise of the free-surface, which remained below the pipe crown. After the front passed the free-surface rose gradually as the downstream tank filled (Fig. 3c). The free-surface rise occurred with a more or less uniform rise-rate

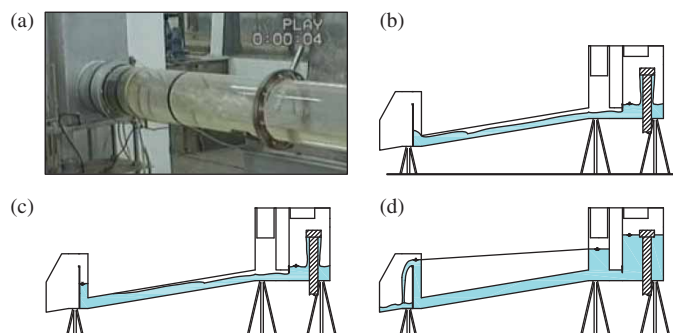


Figure 3 Smooth pressurization: (a) formation of a front not reaching the pipe crown; (b) propagation upstream of the bore without pipe pressurization; (c) backward pressurization as the downstream tank filled and (d) new steady flow after pipe pressurization

along the pipe until the pipe pressurized, starting from the downstream end. Before pipe pressurization concluded, the bore had reached the upstream tank, which had begun to fill and submerge the pipe inlet. Eventually, a moderate amount of air remained entrapped in the form of a long and thin air pocket, sometimes longer than half a pipe length, between the rising liquid surface and the pipe crown. The pocket then split into smaller ones, each a few metres long, which migrated upstream to be finally released through the tank. When the overflowing flow rates in the upstream and downstream tanks equalled the entering flow rate  $Q$ , pipe pressures stabilized at the new steady flow values (Fig. 3d). Because this transient pattern caused pipe pressurization by gradual rising of the free-surface, we called it "smooth" pressurization (Ciraolo and Ferreri 2007). An analogous pressurization pattern relating to experiments with low flow rates was described by Cardle et al. (1989). Numerical simulation of smooth pressurization observed in our runs was studied by Ferreri et al. (2010).

Figure 4 shows, as an example, the chronological diagrams of the pipe-invert pressure heads in sections of transducers 1–5 relating to the smooth pressurization of run II.B.15 (cycle II, group B, flow rate  $Q = 15 \text{ dm}^3 \text{ s}^{-1}$ ). The horizontal broken line indicates the pipe crown. The passing of the front (Fig. 3b) is easily identifiable from the sudden pressure increase; the total pressure (i.e. the flow depth plus the front height) did not reach the pipe crown. The times at which the front reached the transducer sections indicate a nearly constant celerity. The next first ascending stretch, which mirrors the downstream tank filling (Fig. 3c), refers to pipe pressurization; nearly equal diagram slopes indicate approximately uniform free-surface rise-rate along the pipe. After the front flowed into the upstream tank (time marked by the vertical dotted line), there followed a second ascending stretch with a considerably higher slope because this tank also began filling. At first the filling was faster but then slowed because the spillway began working. Then the stabilization stage of upstream and downstream tank levels is observed in the diagram, during which a relative maximum occurs. This stage is followed by the horizontal stretch of steady pressurized operation (Fig. 3d).

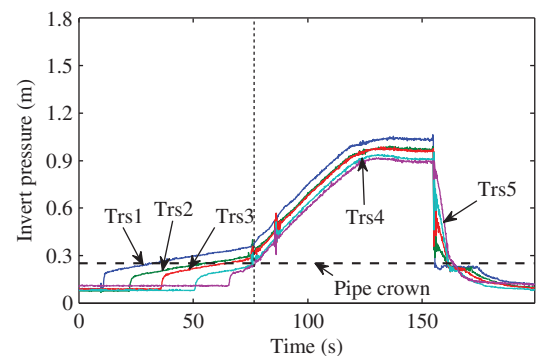


Figure 4 Chronological diagrams of invert pressure at the transducers 1–5 located along the pipe relating to smooth pressurization of run II.B.15 (cycle II, group B, flow rate  $Q = 15 \text{ dm}^3 \text{ s}^{-1}$ ); the dotted line marks the time when the front flowed into the upstream tank

Finally, the decreasing stretch of the diagrams refers to pipe depressurization. More intense oscillations than in the remaining part of the run occurred for short lapses of time, generally during the second ascending stretch.

As the flow rate increased, the front intensity grew, and the front itself became increasingly definite and foamy. The level in the downstream tank first reached and then exceeded the pipe crown, and, consequently, the front completely filled the pipe cross-section (Fig. 5a). The pipe therefore began to pressurize starting from downstream, and along the entire pipe the passing of the front caused quasi-instantaneous pressurization of the cross-section just reached by the front itself (Fig. 5b). While advancing, the front entrained some air in the form of a swarm of little bubbles, which was swept behind the front itself and gathered on the pipe crown (Fig. 5c), where pockets formed (usually only one). Pockets were some metres long and in several cases reached 6–8 m; they were more or less thick, depending on the free-surface flow characteristics. These pockets were followed by some minor pockets (generally a few centimetres long but sometimes up to decimetres). Generally, the largest pockets were released through the upstream tank after pressurization ended, whereas the smaller pockets were swept downstream to be released through the downstream tank. Pressurization ended when the front reached the pipe inlet at the upstream tank. At this time, a temporary pressure drop occurred in the pipe (Fig. 5d) as the water level in the upstream tank was still practically unchanged. After the front flowed, the tank began to fill until the new steady flow conditions were reached (Fig. 3d). The tank filling caused submerging of the pipe inlet, which hindered air pocket release. Because this pressurization type involved quasi-instantaneous pressurization of each cross-section when reached by the bore front, we called it “abrupt” pressurization (Ciraolo and Ferreri 2007).

Figure 6 shows, as an example, the experimental results relating to abrupt pressurization of run V.A.50 (cycle V, group A, flow rate  $Q = 50 \text{ dm}^3 \text{ s}^{-1}$ ); once again, the horizontal broken line indicates the pipe crown. The figure reports the pressure diagrams recorded in transducer sections 2–5: Fig. 6a compares all

diagrams, whereas Fig. 6b–e report the diagrams of sections 2–5 one by one. The front passing (Fig. 5b) is easily identifiable from the sudden pressure increase. Figure 6a shows that the front advanced with a nearly constant celerity while its intensity slightly decreased. The front pressure step is followed by a first temporary pressure drop (more noticeable in transducers 2, 3 and 4; Fig. 6b–d). This drop is probably due to the passing, through the zone behind the front, of a swarm of little bubbles (still having quasi-atmospheric pressure) just entrained by the advancing front itself (Fig. 5c), as shown by the film clips. The next first ascending stretch, which mirrors the downstream tank filling, refers to pipe pressurization (Fig. 5b and 5c). The front flowing into the upstream tank is revealed by a second temporary pressure drop (Fig. 5d), which in Fig. 6a–e is marked by a vertical dotted line, and it is more visible in the single transducer diagrams relating to the more upstream sections (Fig. 6c–e). There follows a second ascending stretch, relating to the upstream tank filling, which once again was at first faster but then slowed because of the spillway. The ensuing stabilization stage of the levels in the upstream and downstream tanks (during which a relative maximum occurred) and the steady pressurized operation (horizontal stretch) are shown. Finally, the decreasing stretch of the diagrams refers to pipe depressurization.

Smooth pressurization was only observed in the runs having flow rate  $Q \leq 20 \text{ dm}^3 \text{ s}^{-1}$ , for all the positions, A, B and C, of the movable wall; such flow rates concerned cycles I and II only

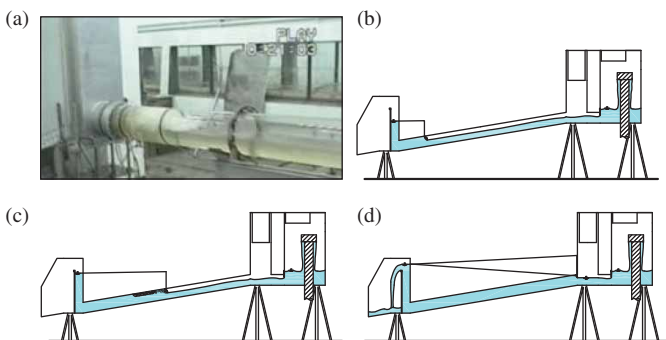


Figure 5 Abrupt pressurization: (a) formation of a front filling the whole pipe section; (b) quasi-instantaneous pressurization of a pipe cross-section as it was reached by the front; (c) formation of large air pockets due to progressive accumulation of air entrained by the front and (d) temporary pressure drop in the whole pressurized pipe as the front flowed into the upstream tank

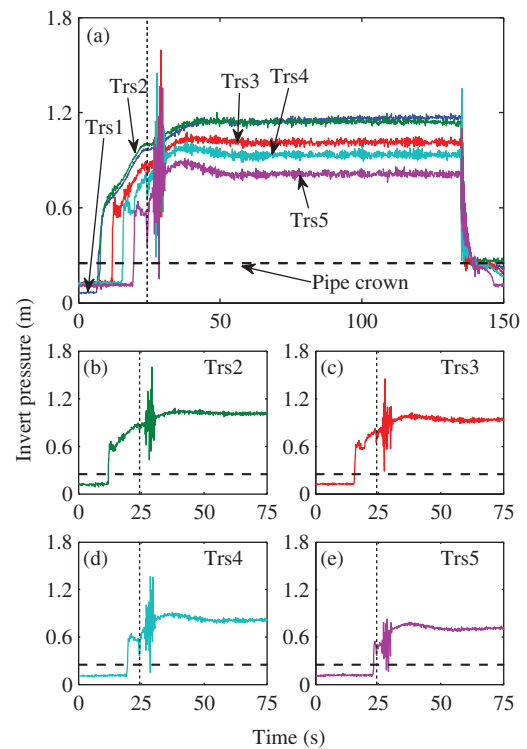


Figure 6 Chronological diagrams of invert pressure at transducers 1–5 located along the pipe relating to abrupt pressurization of run V.A.50 (cycle V, group A, flow rate  $Q = 50 \text{ dm}^3 \text{ s}^{-1}$ ): (a) collective comparison of all transducer diagrams and (b–e) diagrams of single transducers 2–5, respectively

(see Table 1). In all the runs having flow rates  $Q \geq 25 \text{ dm}^3 \text{ s}^{-1}$ , only abrupt pressurization was observed. The important topic of the physical factors (namely, flow rate and depth), which in a given sewer (diameter, slope and roughness) determine either smooth or abrupt pressurization, is stressed in Ferreri et al. (2014). The authors showed by a theoretical approach that, as the flow rate exceeds a characteristic flow rate  $Q_{max}^*$ , dependent on the pipe diameter only, only abrupt pressurization can occur. For the diameter  $D = 244 \text{ mm}$  of the present testing,  $Q_{max}^* = 23.2 \text{ dm}^3 \text{ s}^{-1}$ , which is consistent with our experimental evidence.

### 3.2 Pressure oscillations

Two different pressure oscillation types are discernible in the experimental diagrams, as stated by Ciruolo and Ferreri (2007). The first type appeared during the whole recording time (steady flow included) and had moderate amplitude only; these oscillations were imputable to transducer background noise and flow turbulence and therefore were not considered. In contrast, the second type appeared only for a few limited lapses of time (sometimes only one) during unsteady flow; these oscillations are those indicated in the literature as water-hammer oscillations, and could have either “low” (Fig. 4) or “high” (Fig. 6a) amplitude, depending on the run characteristics. Low oscillations were noticeable in practically all the runs (with smooth or abrupt pressurization), both before and after the front flowed, but they seemed not to be dangerous for sewer stability, despite scale effects between the laboratory model and field situations. High amplitude oscillations, by contrast, were observed in abrupt pressurization only and generally occurred after the whole pipe had been pressurized, with several exceptions in which such oscillations began before the front flowed into the upstream tank (discussed later). These high oscillations may be dangerous for sewer stability.

A comparative examination of all the results of our runs led us to conclude that pressure oscillations were imputable to the pulsations of air pockets entrapped in the liquid flow. These pulsations generally occurred during (a) the pocket growth by gathering air captured by the front, (b) pocket migration towards the upstream tank following the front and (c) during pocket release through the upstream tank. Because pockets were several metres long, their release involved “migration” of the long volumes. In particular, high oscillations were caused by the pulsations of pockets during their migration-release process. The latter interpretation, corroborated by direct observation of the runs and close examination of the film clips, is based on the following considerations: (1) the experimental diagrams show that such oscillations generally occurred after the front outflow, which is revealed by the temporary pressure drop in the pipe pressure diagrams as well as by a sudden rise in the upstream tank diagram (not reported here); (2) high oscillations particularly affected transducers Trs2, Trs3, Trs4 and Trs5 located in the pipe section run through by air pockets during their migration and

release, and they disappeared when the pockets had been completely released; (3) only low oscillations occurred when not much air was entrapped in the liquid flow, as in smooth pressurization and in several runs with abrupt pressurization (discussed later). The explanation of pressure oscillations as a consequence of the air pocket migration-release process is further confirmed by the issues of the mathematic modelling carried out in previous works (Ciruolo and Ferreri 2008a, 2008b).

For practical purposes, major interest is in high oscillations, and therefore from this point on we only address abrupt pressurization.

### 3.3 Analysis of the whole runs

Comparative examination of all the diagrams of abrupt pressurization runs allows us to draw some general conclusions. In most runs the front advanced along the pipe with a nearly constant absolute celerity while its intensity decreased. For fixed position ( $A, B$  or  $C$ ) of the movable wall and pipe slope  $S_0$ , as the flow rate  $Q$  increased (Fig. 7a–d), the front intensity and the front celerity increased considerably. The celerity increase was due to the more rapid pipe filling, whereas the intensity increase was due to an increase in the momentum entering the fluid column already pressurized. As the front advanced, no noticeable variations in the front intensity decrease are clearly visually distinguishable in the diagrams from one run to another, also because of the presence of oscillations. Moreover, an increase in  $Q$  also caused a noticeable increase in the slope of the ascending stretch following the front because of the more rapid downstream tank filling; this stretch continued until either the front flowing or the downstream spillway overflow occurred.

For a fixed movable wall position and flow rate  $Q$ , as the pipe slope  $S_0$  increased (Fig. 8a–d), the absolute front celerity decreased noticeably, mainly because of the increase in the free-surface flow velocity  $V_1$ . Moreover, in each section the front intensity exhibited a slight increase due to the increase in the momentum entering the fluid column. An increase in the front

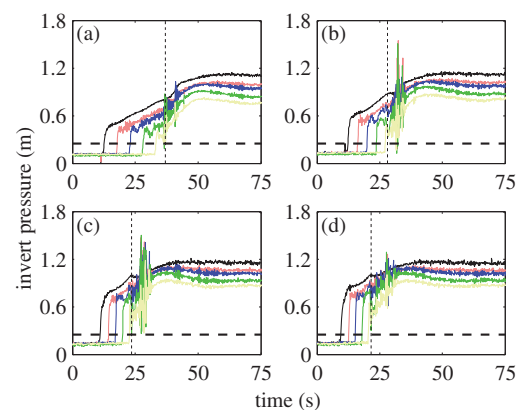


Figure 7 Comparison of experimental diagrams for fixed pipe slope ( $S_0 = 1.5\%$ ) and movable wall position ( $A$ ) as the flow rate  $Q$  increased: (a) run IV.A.40 (i.e. cycle IV, group A, flow rate  $Q = 40 \text{ dm}^3 \text{ s}^{-1}$ ); (b) run IV.A.50; (c) run IV.A.55 and (d) run IV.A.60

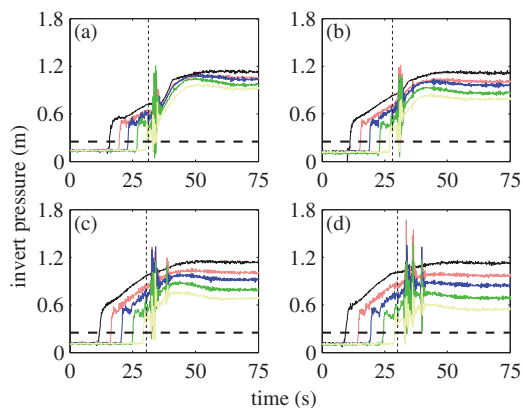


Figure 8 Comparison of experimental diagrams for fixed flow rate ( $Q = 45 \text{ dm}^3 \text{ s}^{-1}$ ) and movable wall position  $A$  as the pipe slope  $S_0$  increased: (a) run III.A.45 (i.e. cycle III, group A, flow rate  $Q = 45 \text{ dm}^3 \text{ s}^{-1}$ ); (b) run IV.A.45; (c) run V.A.45 and (d) run VI.A.45

intensity drop along the pipe is clearly distinguishable as an immediate effect of pipe-invert rising. The pipe-invert rising also caused a decrease in the final steady pressures in each section. The slope of the ascending stretch following the front increased because of more rapid downstream tank filling.

General conclusions for pressure oscillation peculiarities are more difficult to formulate than for other transient characteristics because of the complexity and variety of the air–water interaction phenomena occurring. Low oscillations were observed in all the runs, whereas high oscillations were observed only in the runs with a flow rate  $Q \geq 35 \text{ dm}^3 \text{ s}^{-1}$ . For a fixed position ( $A$ ,  $B$  or  $C$ ) of the movable wall and pipe slope  $S_0$ , as the flow rate  $Q$  increased (Fig. 7a–d), the high oscillation amplitude generally first increased but then decreased. Once such oscillations are imputed to the pulsations of air pockets during their migration–release, this behaviour is explained as follows. As  $Q$  increased, the front intensity and celerity increased; however, both the front cross-section (through which air was entrained in the pressurized water column) and air present in the pipe decreased. These physical facts involved variation in the air pocket characteristics (mass, length, thickness and migration speed) on which the pulsation characteristics depended (Ciraolo and Ferreri 2008b). It is likely that a maximum for entrapped air mass was reached, but no specific measurements were taken. The dependence of oscillation characteristics on air pocket characteristics is consistent with the results of Zhou *et al.* (2002a) and of Vasconcelos and Write (2005).

For a fixed movable wall position and flow rate  $Q$ , a general growth in the oscillation intensity occurred as the pipe slope  $S_0$  increased (Fig. 8a–d). A physical explanation for this trend is an increase in air entrainment caused by the flow depth  $y_1$  decrease, which produced increases in both pipe air and the front cross-section, as well as an increase in the momentum entering the fluid column (the latter two caused an increase in the front turbulence and air entrainment). This trend, however, occurred until  $Q = 55 \text{ dm}^3 \text{ s}^{-1}$ . For  $Q > 55 \text{ dm}^3 \text{ s}^{-1}$  (i.e.  $Q = 60$  and  $65 \text{ dm}^3 \text{ s}^{-1}$ ), no trend was discernible in our results because the higher flow

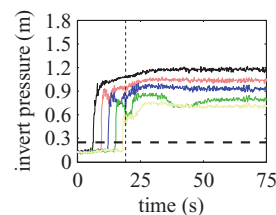


Figure 9 Results of run VI.A.65 (cycle VI, group A, flow rate  $Q = 65 \text{ dm}^3 \text{ s}^{-1}$ ) in which only low oscillations occurred despite a large amount of air captured by the front, because the air pocket was entrapped and there was no release

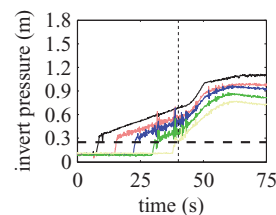


Figure 10 Results of run IV.A.30 (cycle IV, group A, flow rate  $Q = 30 \text{ dm}^3 \text{ s}^{-1}$ ) in which formation of only low oscillations was observed because only a small amount of air was captured and it was easily released through the upstream tank

depths,  $y_1$ , combined with the other run characteristics caused different behaviours from one run to another. In cycle VI, for example, only a minor part of the single air pocket (about 6 m long and half a diameter thick) was released, whereas, because of the rapid filling of the upstream tank and the consequent head over the pipe inlet, most of the air was steadily entrapped between the pipe inlet itself and the full-pipe section flow. The absence of release resulted in no high oscillations being observed (Fig. 9), despite a large amount of air being captured by the front.

Abrupt pressurization with low oscillations only occurred in runs with flow rates  $Q = 25$  and  $30 \text{ dm}^3 \text{ s}^{-1}$ . As an example, Fig. 10 shows the diagrams of run IV.A.30. The front characteristics did not allow a large amount of air to be captured in the liquid flow, and most of the air was released before the tank water level went considerably over the pipe inlet. The examination of the upstream tank diagrams (not reported here) shows that for  $Q < 35 \text{ dm}^3 \text{ s}^{-1}$ , the sudden rise in the tank level caused the latter to either not reach the inlet-pipe crown or to not exceed it by much (i.e. when the front flowed, the release of the following air pocket started either before the pipe inlet was wholly submerged or when the pipe inlet dip was still low); in contrast, for  $Q \geq 35 \text{ dm}^3 \text{ s}^{-1}$  the sudden level rise always produced a noticeable pipe inlet dip. The occurrence of either high or only low oscillations therefore did not depend on the pressurization pattern only, but also on the upstream manhole geometric characteristics, in particular the plant size, on which level rise-rate depended.

Unusual behaviours were observed in a few runs, such as in the runs of cycle III ( $S_0 = 1\%$ ) having the highest flow rates ( $60$  and  $65 \text{ dm}^3 \text{ s}^{-1}$ ). Figure 11, relating to run III.A.65, shows that at about the same time the front reached transducer 3 (Fig. 11a), a sudden and noticeable increase in the pressure at transducer 4 occurred (Fig. 11b), and the upstream tank filling started



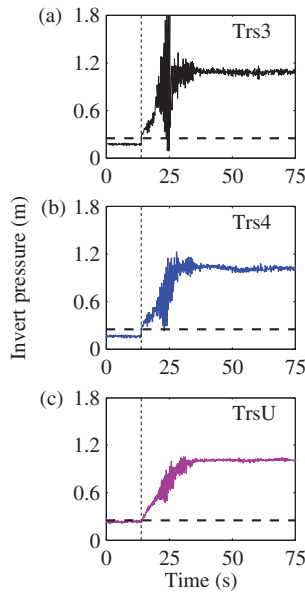


Figure 11 Results of run III.A.65 (cycle III, group A, flow rate  $Q = 65 \text{ dm}^3 \text{ s}^{-1}$ ) in which oscillations having higher intensity and longer duration than in other runs occurred before the front flowed due to early upstream tank filling: (a) pressure diagram at transducer 3; (b) synchronic sudden increase in the air pressure at transducer 4, without being reached by the front and (c) synchronic start of upstream tank filling diagram

(Fig. 11c). Aided by the film clip, we concluded that the high front celerity caused a noticeable increase in air pressure ahead of the front itself, which produced a temporary decrease in the flow rate entering the pipe and a slowing of the front until it stopped. The consequent rapid tank filling caused the pipe inlet to be submerged before the front reached the inlet itself, and an air pocket was entrapped between the front and the submerged inlet. Then, as the head in the upstream tank became high enough, the pocket broke through the front and joined up with the pocket of entrained air behind the front itself. The large pocket was then dragged slowly downstream. However, the pocket pulsations during stages of pocket entrapment and the front breaking through and joining up produced considerable oscillations as well (Fig. 11a).

Regarding the movable wall position (A, B or C), comparison between the results relating to the same slope and flow rate values did not reveal noticeable differences on the qualitative plane. Figure 12 shows, as an example, the results of the three runs of cycle III having flow rate  $Q = 50 \text{ dm}^3 \text{ s}^{-1}$ . Pressure oscillations were analogous, and the most noticeable difference was the large increase in the final steady pressures concerning position C due to the considerable increase in the steepness of the downstream tank discharge curve; in this respect, even in the runs of group C, the previously mentioned imperfect wet seal of the movable wall allowed a noticeable part of the flow rate  $Q$  to be discharged through the downstream tank. Direct observation and film clip examination of the runs allowed us to discern a more “regular” processes of air entrainment by the front advancing and of air release through the upstream tank as the wall position moved back from A to C.

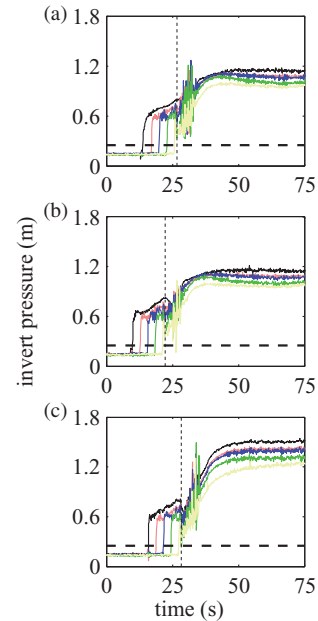


Figure 12 Comparison of experimental results for fixed pipe slope ( $S_0 = 1\%$ ) and flow rate ( $Q = 50 \text{ dm}^3 \text{ s}^{-1}$ ) as the position of the movable wall changed: (a) position A; (b) position B and (c) position C

#### 4 Discussion of results

Examination of the tests led us to draw several conclusions, some of which are in agreement with the previous literature findings whereas others give a different description or interpretation of some aspects of the transient. Such differences may even arise from the peculiarities of the experimental equipment, of run execution or of the run characteristics (flow rate, filling ratio, etc.) used by each researcher. In this respect, the different scaling of the various phenomena involved in pipe pressurization as the pipe size changes must be considered.

Our tests showed that either smooth or abrupt pressurization could occur; the latter was observed for the flow rates  $Q \geq 25 \text{ dm}^3 \text{ s}^{-1}$  only. The existence of two pressurization patterns is consistent with the observations by Hamam and McCorquodale (1982) and Cardle *et al.* (1989) who, however, did not study the occurrence of one pattern or the other.

Intense pressure oscillations, which mostly concern sewer stability, were observed by us in abrupt pressurization only. Close examination and comparison of all the experimental diagrams and close observation of each related film clip allowed us to state that, except for a few experimental situations, intense oscillations occurred after the front flowed into the upstream tank, and that they were generated by pulsating of air pockets during their migration along the pipe and their release through the upstream tank. These results differ from those of previous researchers who experimentally studied abrupt pressurization (Hamam and McCorquodale 1982, Cardle *et al.* 1989, Aimable and Zech 2003). According to these studies, pressure oscillations

started before the front flowed into the upstream tank and vanished when the front flowed (Cardle *et al.* 1989); in particular, oscillations started when an air pocket was entrapped between the advancing front and a wave reaching the pipe crown, which was produced by the evolution of free-surface instability produced by the “wind” driven by the front itself. Therefore, in this interpretation the oscillation source was the front itself as it advanced pushing the air pocket. In our experiments we never observed any free-surface instability having analogous evolution, and air pockets formed in water flow because of progressive accumulation of air entrained by the foamy front as it advanced, not because of air entrapment. This difference is likely because the previous experiments were performed using filling ratios higher than the limit value 0.81 for which any instability may grow up to the pipe crown, whereas our filling ratios were less than this limit (in one case only it was  $y_1/D = 0.79$ ). It therefore follows that abrupt pressurization can occur following, in turn, two different patterns according to whether the initial filling ratio is either higher or lower than the instability limit 0.81.

A linked question concerns oscillation intensity. Our runs showed that, generally, (a) the larger the air pocket, the higher the oscillations, and that (b) the harder the air release, the higher the oscillations; therefore, oscillations intensity arose from the combination of situations (a) and (b). These results are consistent with those of Vasconcelos and Wright (2005) and Zhou *et al.* (2002a, 2002b) who noted that pressure oscillation characteristics are greatly affected by the amount of air and the release modalities. As the filling ratio exceeds 0.81, the air amount present in the pipe is rather low, but the differences between the realization patterns leave the question open as to which abrupt pressurization pattern produces higher oscillations. In fact, pressure oscillations shown in Hamam and McCorquodale (1982) and Cardle *et al.* (1989) seem to be less intense (their intensity is similar to the front height) and less persistent than ours.

Another difference shown by our tests is the behaviour of the front as it advanced. In our runs, where air pockets followed the front, the front intensity slightly decreased. In contrast, in the runs by Cardle *et al.* (1989) in which the air pocket was driven by the front, the front intensity increased as the front itself increasingly pushed the air pocket.

Note that pressure oscillations studied both by us and in previous works, with a pipe between two ventilated tanks, were produced by the interaction between the liquid flow and air entrapped, through different mechanisms. In real cases with unvented manhole covers, both air already present in the manholes and air captured by the liquid flow during pressurization cannot flow out from the manholes themselves. In such cases, dynamic interaction between the total entrapped air and water flow may subsequently result in considerably higher oscillations than for well-ventilated drainage systems.

Finally, considering the previous findings, we note the following. Pressure oscillations occurring during pipe pressurization are often indicated in the technical literature as a *water-hammer* phenomenon. However, this idiom refers to oscillations directly

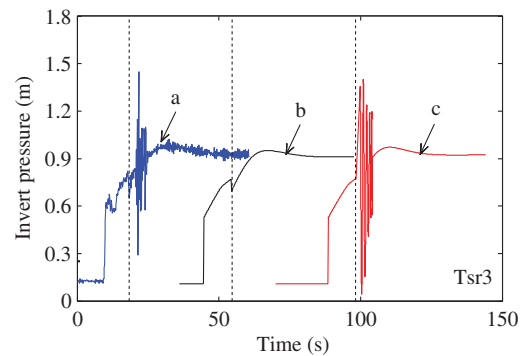


Figure 13 Comparison for run V.A.50 (cycle V, group A, flow rate  $Q = 50 \text{ dm}^3 \text{ s}^{-1}$ ), of (a) the experimental surge at transducer 3; (b) the mean surge simulated by a rigid-column method by Ciruolo and Ferreri (2008a); and (c) the surge with oscillations simulated by Ciruolo and Ferreri (2008b) considering a pulsating air pocket

produced by the changes in water velocities consequent on the downstream obstruction, whereas in pipe pressurization they are only indirectly produced by these changes through the pulsations of air entrained. Numerical simulations by Ciruolo and Ferreri (2008a) (Fig. 13) showed that, in a ventilated pipe, the “mean” experimental surge (i.e. the surge filtered out of the oscillations) was well reproduced by a rigid-column method, which accounted for water velocity changes but ignored the presence of air pockets. Other numerical simulations by Ciruolo and Ferreri (2008b) (Fig. 13) showed that, as an air pocket having suitable characteristics (volume, length, *etc.*) was put inside the water flow, its pulsations as it migrated upstream yielded pressure oscillations around the mean surge analogous to the measured ones. In summary, provided a sewer is well ventilated, pressure oscillations are a manifestation of a “side” phenomenon (air pocket pulsation) within the “main” water flow transient (pipe and tank filling); therefore, more generic idioms such as “transient” or “unsteady flow” seem to be more appropriate than “water-hammer”.

## 5 Conclusions

Sewer pressurization transient, a frequent phenomenon in urban drainage systems but currently little understood, was examined experimentally. Pressurization was explored through 144 experimental runs covering wide ranges of flow rates and pipe slopes and, unlike experiments found in the technical literature, situations involving considerable participation of air and more intense pressure oscillations were also reproduced. The experimental investigation resulted in extensive information on the phenomenon.

Two distinct pressurization patterns, denoted by us as “smooth” and “abrupt”, were observed according to whether the front produced by the closing operation either did not reach (smooth) or went over (abrupt) the pipe crown, but only the latter could produce intense pressure oscillations and was therefore examined more closely.

Abrupt pressurization occurred according to a different pattern from that known in the literature, as no free-surface instability rising up to the pipe crown and consequent air pocket entrapment were observed. By contrast, large air pockets could form inside the liquid flow because of progressive accumulation of air entrained by the foamy front as it advanced.

With a few exceptions, pressure oscillations generally occurred for a few short lapses of time after the front flowed into the upstream tank. Oscillations were generated by the pulsations of air pockets as they were released through the upstream tank. Contrary to findings reported in the literature, no direct connection of pressure oscillations with front formation and advancement was observed. Oscillation time and production mechanism differed from those described for abrupt pressurization by previous researchers who deliberately carried out experiments with filling ratios falling within a range of free-surface flow instability. In our experiments the oscillation intensity generally increased with the amount of air in the pockets and the difficulty of release, both depending on the characteristics of the free-surface flow, namely the flow rate and the pipe slope.

Based on these results, precautions for pressure oscillation control should aim at limiting air pocket accumulation as well as at facilitating pocket release. The next research step should concern reliable numerical modelling of the whole surge, oscillations included.

### Acknowledgements

The writers wish to thank Dr Dora Ferreri and Dr Emanuele Di Lucia who, with dedication and systematic work, carried out the experiments and made the measurements, and finally placed the latter at our disposal, as well as Dr Salvatore Falzone, who effectively collaborated in numerical simulations which helped the writers in better interpreting the experimental diagrams.

### Notation

$A_1$	=	free-surface flow cross-sectional area ( $\text{m}^2$ )
$B_1$	=	free-surface flow width (m)
$D$	=	pipe diameter (mm)
$F_1$	=	free-surface flow Froude number (—)
$g$	=	gravity acceleration ( $\text{m s}^{-2}$ )
$Q$	=	flow rate ( $\text{dm}^3 \text{s}^{-1}$ )
$S_0$	=	pipe slope (%)
$V_1$	=	free-surface flow velocity ( $\text{m s}^{-1}$ )
$y_1$	=	free-surface flow depth (m)

### References

Aimable, R., Zech, Y. (2003). Experimental results on transient and intermittent flows in a sewer pipe model. Proc. 30th IAHF Congress, Thessaloniki, Greece, B, 377–384.

- Capart, H., Sillen, X., Zech, Y. (1997). Numerical and experimental water transients in sewer pipes. *J. Hydraulic Res.* 35(5), 659–670.
- Cardle, J.A., Song, C.C.S., Yuan, M. (1989). Measurement of mixed transient flows. *J. Hydraulics Div.* 115(2), 169–182.
- Ciraolo, G., Ferreri, G.B. (2007). Experimental investigation on pressurization transient of a drainage sewer. Proc. 5th Int. Symp. *Environmental hydraulics – ISEH V*, Tempe, Arizona. <http://www.iahr.net/iseh/home/>, on CD-ROM, 1–6.
- Ciraolo, G., Ferreri, G.B. (2008a). Sewer pressurization modelling by a rigid-column method. Proc. 11th Int. Conf. *Urban drainage – 11th ICUD*, Edinburgh, Scotland. <http://www.11icud.org/>, on CD-ROM, 1–10.
- Ciraolo, G., Ferreri, G.B. (2008b). Mathematical modelling of pressure oscillations in sewer pressurization. Proc. 11th Int. Conf. *Urban drainage – 11th ICUD*, Edinburgh, UK. <http://www.11icud.org/>, on CD-ROM, 1–10.
- Ferreri, G.B., Freni, G., Tomaselli, P.D. (2010). Ability of Preissmann slot scheme to simulate smooth pressurization transient in sewers. *Water Sci. Technol.* 62(8), 1848–1858.
- Ferreri, G.B., Ciraolo, G., Lo Re, C. (2014). Flow hydraulic characteristics determining the occurrence of either smooth or abrupt sewer pressurization. *J. Hydraulic Res.* 52.
- Guo, Q., Song, C.C.S. (1990). Surging in urban storm drainage systems. *J. Hydraulic Eng.* 116(12), 1523–1537.
- Guo, Q., Song, C.C.S. (1991). Dropshaft hydrodynamics under transient conditions. *J. Hydraulic Eng.* 117(8), 1042–1055.
- Hamam, M.A., McCorquodale, J.A. (1982). Transient conditions in the transition from gravity to surcharged sewer flow. *Can. J. Civil Eng.* 9(2), 189–196.
- Li, J., McCorquodale, J.A. (1999). Modelling mixed flow in storm sewers. *J. Hydraulic Eng.* 125(11), 1170–1180.
- Song, C.C.S. (1976). Two-phase flow hydraulic transient model for storm sewer systems. Proc. Int. Conf. *Pressure surges*, BHRA Fluid Engineering, Cranfield, Bedford, 17–34.
- Song, C.C.S., Cardle, J.A., Leung, K.S. (1983). Transient mixed flow models for storm sewers. *J. Hydraulics Div.* 109(11), 1487–1504.
- Trajkovic, B., Ivetic, M., Calomino, F., D'Ippolito, A. (1999). Investigation of transition from free surface to pressurized flow in a circular pipe. *Water Sci. Technol.* 39(9), 105–112.
- Vasconcelos, J.G., Wright, S.J. (2005). Experimental investigation of surges in a stormwater storage tunnel. *J. Hydraulic Eng.* 131(10), 853–861.
- Wiggert, D.C. (1972). Transient flow in free-surface, pressurized systems. *J. Hydraulics Div.* 98(HY1), 11–27.
- Zhou, F., Hicks, F.E., Steffler, P.M. (2002a). Transient flow in a rapidly filling horizontal pipe containing trapped air. *J. Hydraulic Eng.* 128(6), 625–634.
- Zhou, F., Hicks, F.E., Steffler, P.M. (2002b). Observations of air–water interaction in a rapidly filling horizontal pipe. *J. Hydraulic Eng.* 128(6), 635–639.